Engineering Geology 264 (2020) 105331

Contents lists available at ScienceDirect

Engineering Geology

journal homepage: www.elsevier.com/locate/enggeo

Completeness Index for Earthquake-Induced Landslide Inventories

Tanyas Hakan[a,b], Lombardo Luigi[c,*]

[a] NASA Goddard Space Flight Center, Hydrological Sciences Laboratory, Greenbelt, MD, USA
[b] USRA, Universities Space Research Association, Columbia, MD, USA
[c] University of Twente, Faculty of Geo-Information Science and Earth Observation (ITC), PO Box 217, Enschede, AE 7500, Netherlands

ARTICLE INFO

Keywords:
Earthquake-Induced Landslides
Landslide Inventory
Landslide-Affected Area
Landslide-Susceptible Area
Completeness Index

ABSTRACT

Understanding the global relation between Earthquake-Induced Landslides (EQILs) and the factors contributing to their initiation is still an open topic within the geomorphological community. Accessing EQIL inventories and analyzing them concerning their potential causes is the key to explore such relation. However, each of the existing EQIL inventories has its level of completeness and associated uncertainty which makes any unified relationship which is challenging to obtain. So far, the completeness of EQIL inventories has never been clearly defined. As a result, it has never been accounted for in global EQIL predictive models. In this technical note, we propose a simple definition for the completeness of EQIL inventories. We analyze 30 digital EQIL for 21 earthquakes and develop a semi-quantitative method to estimate the completeness level, which we refer to as Completeness Index (CI). The CI results from a combination of topographic factors, ground shaking parameters, and a measure derived from landslide size statistics. The proposed CI consists of Low, Moderate, and High completeness classes which can be used to evaluate any landslide inventory.

We made the whole procedure to compute the CI accessible in an ArcGIS toolbox together with a test dataset (see supplementary material).

1. Introduction

Two terms exist to assess the reliability of a landslide inventory: quality and completeness. The quality of an inventory is defined based on geographical and thematic accuracy of the information shown on a map (Guzzetti et al., 2012). The completeness represents the extent to which an EQIL inventory includes all co-seismic landslides for a specific earthquake (Guzzetti et al., 2012). Both quality and completeness directly affect the reliability of landslide susceptibility (*e.g.,* Lombardo and Mai, 2018), intensity (*e.g.,* Lombardo et al., 2019a) and hazard assessments (*e.g.* Pellicani and Spilotro, 2015) or, more generally, any other analysis involving the size, type and spatial distribution of landslides (Fell et al., 2008). The quality and completeness of an inventory also affect the Landslide-Event Magnitude scale (Tanyaş et al., 2019), which is used to quantify any landslide event (Keefer, 1984; Malamud et al., 2004; Tanyaş et al., 2018). Estimating the quality is generally not achievable because sufficient background information regarding the mapping procedure is not provided (Tanyaş et al., 2017).

Although the limitations due to poor metadata still apply for completeness, few examples still exist in the literature where authors have evaluated the completeness up to some extent. For instance, a qualitative completeness assessment is provided by comparing several inventories pertaining to the same earthquake in *Xu et al.* (*2014b*). However, such a definition of completeness has been proposed only in relative terms. In other words, according to the current literature, a completeness level cannot be assigned in case of single inventories. Another example corresponds to Malamud et al. (2004), where the authors examined the Frequency-Area Distributions (FAD; *e.g.,* Pelletier et al., 1997) of four EQIL inventories. Some of the limitations due to the subjectivity of this mapping procedure have been highlighted by *Tanyas et al.* (*2019*).

Tanyaş et al. (2017) propose a questionnaire to preliminary assess the completeness of co-seismic EQIL inventories. They evaluate it by asking the following questions: Q_1) Have pre-existing landslides been removed from the earthquake-induced landslide inventory? Q_2) Is there a minimum size threshold used for mapping landslides? Q_3) Are landslides mapped for the entire landslide-affected area or just for a subregion?

Whether the first question can be addressed, it entirely depends on the information provided by the authors who digitized the inventory in the first place. However, the remaining two questions can be estimated a posteriori, even without metadata. Specifically, we can use a proxy for the minimum landslide size (Q_2) and a proxy for the examined area (Q_3). The first proxy exploits the suggestions made by Malamud et al. (2004), whereas the second one relies on the framework proposed by Tanyaş and Lombardo (2019).

* Corresponding author.

https://doi.org/10.1016/j.enggeo.2019.105331
Received 1 August 2019; Received in revised form 4 October 2019; Accepted 5 October 2019
Available online 10 November 2019

In this study, we combine such proxies and develop a semi-quantitative evaluation method to assess what we refer to as Completeness Index (CI) for EQIL inventories. As a result, by considering these quantitative proxies, we can express the CI into three qualitative classes: High, Moderate, and Low. To test this procedure, we analyze 30 digital landslide inventories from earthquake events that occurred around the globe.

The workflow to obtain the CI has been made accessible as an ArcGIS toolbox in the supplementary material, together with a test dataset.

2. Background

The proxy we used for the minimum landslide size (Q_2 mentioned above) corresponds to the rollover point in landslide Frequency-Area Distributions (Stark and Hovius, 2001; Guzzetti et al., 2002; Van Den Eeckhaut et al., 2007). The rollover point corresponds to the peak of the curve after which the frequency-density value begins to decrease for smaller landslides, in case of non-cumulative landslide FADs (*e.g.,* Ghosh et al., 2012). The FAD is built based on the areal extent of landslides associated with a given earthquake. Malamud et al. (2004) were the first to model the theoretical FAD curves using four nearly-complete inventories. Based on their modeled distribution, Malamud et al. (2004) interpret the divergence from the theoretical FAD curves as an indication of the incompleteness of the observed inventory. However, this approach does not provide any information regarding the level of completeness. Moreover, Tanyaş et al. (2019) argue that the shapes of landslides FADs show large variability. It is, therefore, not possible to define universal curves and evaluate the completeness comparing an inventory's FAD with theoretical curves. The rollover point is considered as the closest estimate for the landslide size at which the inventory can be assumed to be nearly complete. It can, therefore, be used as a proxy for the minimum mapped landslide (Parker et al., 2015; Tanyaş et al., 2017, 2019).

To address the question regarding which area is mapped with respect to the total affected area, we followed the approach suggested by Tanyaş and Lombardo (2019). The authors examine the landslide-affected area in relation to Peak Ground Acceleration (PGA) and topographic conditions. They recognize the minimum PGA encompassing 90% of all landslides associated with 20 EQIL inventories and referred to it as the Common PGA contour, which corresponds to 0.12 g. Based on the 0.12 g boundary, the authors calculated the Areal Coverage of Landslide-Susceptible Area (ACLSA). The ACLSA is defined as the ratio (expressed in percentage) between the total landslide susceptible area and the area covered by the Common PGA contour. This ratio essentially normalizes the area exposed to ground shaking by the terrain where landslide may occur. The latter is expressed as the areal sum of remaining pixels once those pixels with a slope lower than 5 degrees and relief lower than 100 m have been removed. By correlating the ACLSA to the actual landslide-affected areas, they present a global relation between the two parameters. We use this approach as a proxy for the examined area criterion (Q_3 mentioned above).

3. Material

In this work, we exploit the global EQIL inventory database collected and presented by Schmitt et al. (2017) and Tanyaş et al. (2017). It contains 64 digital EQIL inventories for 46 earthquakes with various quality and completeness levels. In the present contribution, we use 30 EQIL inventories from 21 earthquakes filtering out those missing the size information on individual landslides (Fig. 1). Additionally, we also disregard the inventories for which the epicenter is located offshore. We eliminate the second batch of inventories because they previously proved to behave differently from the rest of the sample (Tanyaş and Lombardo, 2019). Ultimately, we also chose to eliminate inventories associated with more than one major shock because their spatial distribution can reflect multiple disturbances.

4. Methodology

To define a complete EQIL inventory, one needs to know the extent up to which landslides have been mapped via orthophotos or satellite scenes (*e.g.,* Van Westen et al., 2008; Wasowski et al., 2011). We refer to the former as landslide affected area and to the latter as landslide-examined area. Theoretically, the landslide affected-area can be defined with a polygon covering all landslides triggered by the corresponding earthquake. As for the landslide-examined area, this information should be reported in inventories' metadata. However, in the vast majority of landslide inventories, the information regarding the landslide examined-area and whether it corresponds to the whole landslide affected-area is often not reported. This may have an implication on the cascading calculations of the predicted landslide affected-area, whose uncertainty propagation has been already discussed in Tanyaş and Lombardo (2019). The only choice that remains to a landslide scientist is inevitably to consider the boundary within which all the mapped landslides fall. Ideally, if landslide -affected and -examined area coincide, then an inventory would be cartographically complete (not taking into consideration the mapped landslide size yet).

In practice, by knowing both the boundaries of landslide -affected and -examined areas, we can compare them and express their ratio as a proxy for the examined area criterion. Notably, in case of a partial inventory, the actual boundary of the landslide-affected area cannot be determined. However, even for inventories compiled by examining the whole affected area, the resolution of the imagery scanned for mapping can still pose a limitation to the minimum size of recognizable landslides.

Here, we assess the CI according to the following steps. We 1) predict the landslide-affected area; 2) calculate the Percentage of Landslide-Examined Area; 3) calculate the rollover point ($\sim$ minimum landslide size); 4) aggregate this information into the Completeness Index. The stepwise procedure and relative terminology are explained and summarized below.

In step 1, we use the relation (see Fig. 2) between Areal Coverage of Landslide-Susceptible Area (ACLSA) and Peak Ground Acceleration (PGA), following the approach presented in Tanyaş and Lombardo (2019). In other words, we estimate the likely areal extent of landslide-affected areas as a function of PGA. This choice may inherit some limitations due to the simplistic assumption made here. However, for a global model, we assume this to be sufficient as also demonstrated by the correlation pattern retrieved in the aforementioned article.

In Fig. 3, we clarify this approach by showing how to estimate the landslide affected area for the 2015 Gorkha example. As a result, the ACLSA corresponds to 69% of the study area, and the estimated landslide-affected area is bounded by the 0.25 g PGA.

In step 2, we compare the landslide-examined area with the landslide-affected area predicted in Step 1. If the extent of the landslide-examined area is not provided in the corresponding paper/report, we fit a polygon which covers all the mapped landslides and uses this one instead. Subsequently, we calculate the ratio (expressed in percentage) between the landslide-examined area and the predicted landslide-affected area. Fig. 4 summarizes this ratio in map form for two Gorkha inventories, again used as a graphical example. The first inventory was provided by Roback et al. (2017), while the second was digitized by *Tanyas* et al. (*2018*). The resulting Percentage of Landslide-Examined Area (PLEA) corresponds to 99% for the first case and 6% for the second one.

At this stage, PLEA does not account for the unmapped small landslides within a specific EQIL inventory. Tanyaş et al. (2019) claim that the rollover point in FADs can be used as the upper-bound estimate of the minimum landslide size, at which the inventory can be assumed to be nearly complete. We want to remind that mapped landslides for a given inventory can extend to much smaller cases. The rollover,

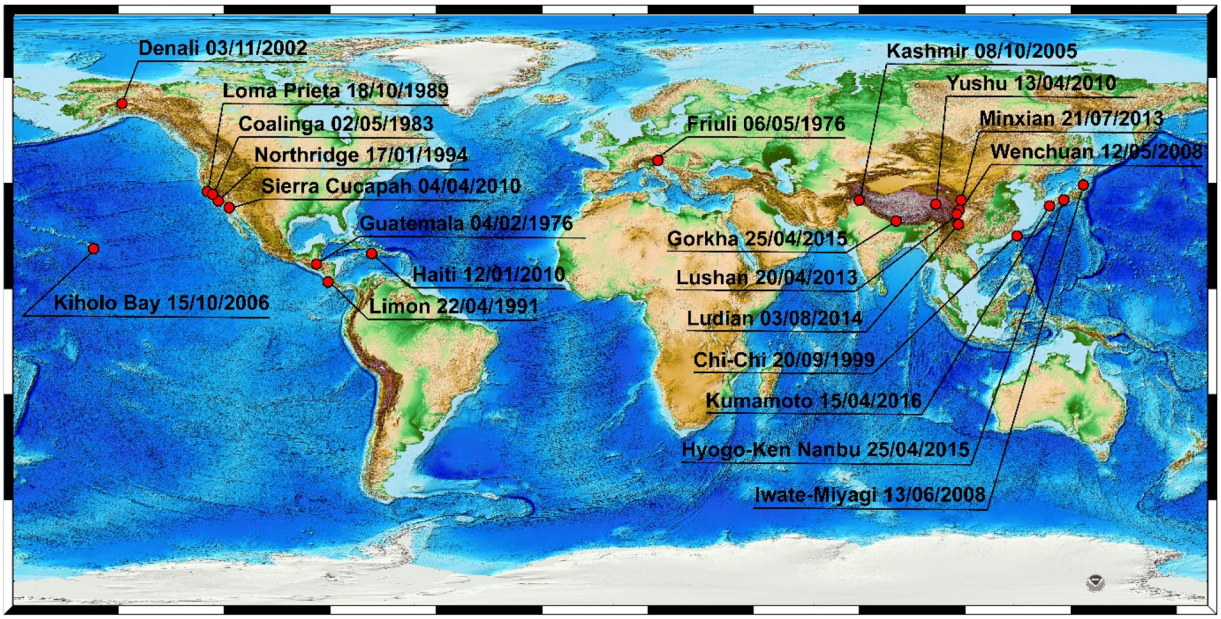

Fig. 1. Locations (and dates) of the 21 global earthquakes used in the present work to test the Completeness Index framework.

however, is interpreted to be representative of a specific class of landslide extents for which their entire distribution is sampled/digitized.

In Step 3, we combine the PLEA with the rollover point information, and the latter used as a proxy for the minimum fully-mapped landslide size.

To put things into perspective, the gold standard for the quality of an EQIL inventory corresponds to the 1994 Northridge inventory (Harp and Jibson, 1995, 1996). This is a rare case, unanimously considered to be nearly-complete (Guzzetti et al., 2002). And, it has already been thoroughly examined by Malamud et al. (2004) when they first proposed the landslide FAD. For this inventory, the rollover point corresponds to ~500 m^2. We consider this value as our reference, and any inventory which deviates from this reference rollover value we assume it to be less detailed.

In step 4, we jointly evaluate the PLEA and rollover size. We simplify the CI into three classes using a combination of these two proxies. EQIL inventories with over 50% PLEA and rollover size equal or smaller than 500 m^2 are classified with "High Completeness" (HC). Those with PLEA greater than 50% but with rollover sizes larger than 500 m^2 are classified with "Moderate Completeness" (MC). And, we classify the inventories which do not satisfy either of the two conditions with "Low Completeness" (LC). Notably, using both PLEA and rollover size produces four combinations. We opted, however, for three classes only because if the percentage of landslide-examined area is low. And no matter the detail at which landsides have been originally mapped, the resulting inventory will still be incomplete.

5. Results

Following steps 1 and 2, we estimate the landslide-affected areas and the PLEA (the latter reported in Fig. 5) for 30 EQIL inventories, respectively. Out of the 30 inventories, the minimum PLEA corresponds to the 2008 Wenchuan inventory published in Tang et al. (2016), whereas six inventories show an average PLEA over 90%. These are the 1983 Coalinga (Harp and Keefer, 1990), the 1994 Northridge (Harp and Jibson, 1995, 1996), the 1999 Chi-chi (Liao and Lee, 2000), the 2008 Wenchuan (Xu et al., 2014b), the 2010 Haiti (Harp and Jibson, 2016), the 2010 Sierra Cucapah (Barlow et al., 2015), the 2013 Lushan (Xu et al., 2015), and the 2015 Gorkha (Roback et al., 2017) EQIL inventories.

According to the third step, we calculate the rollover sizes and report them in Fig. 5. Ultimately, we used these findings to classify each inventory according to the CI (Fig. 5).

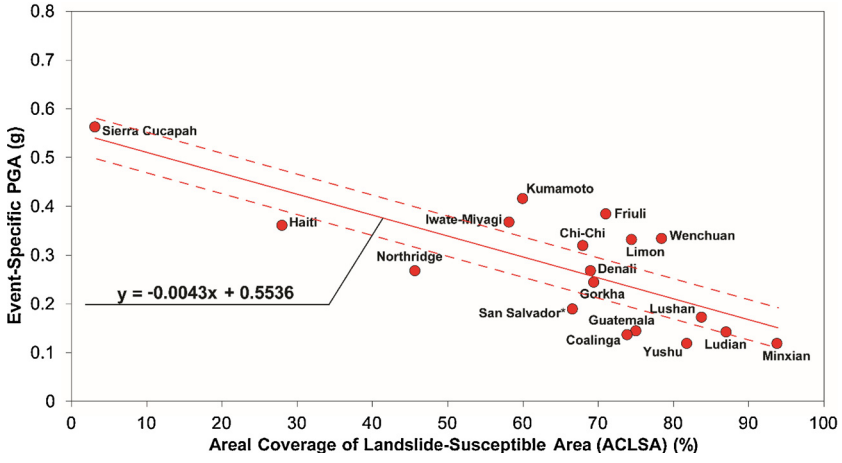

Fig. 2. Relation between ACLSA and the PGA contours (including 90% of all landslides). Figure amended from Tanyaş and Lombardo (2019). The change corresponds to the 1986 San Salvador inventory (Rymer, 1987), which we disregarded in this work because it does not include information on the rollover point. Solid red line corresponds the best linear fit bounded by the associated 95% credible interval, shown in between the dashed lines.

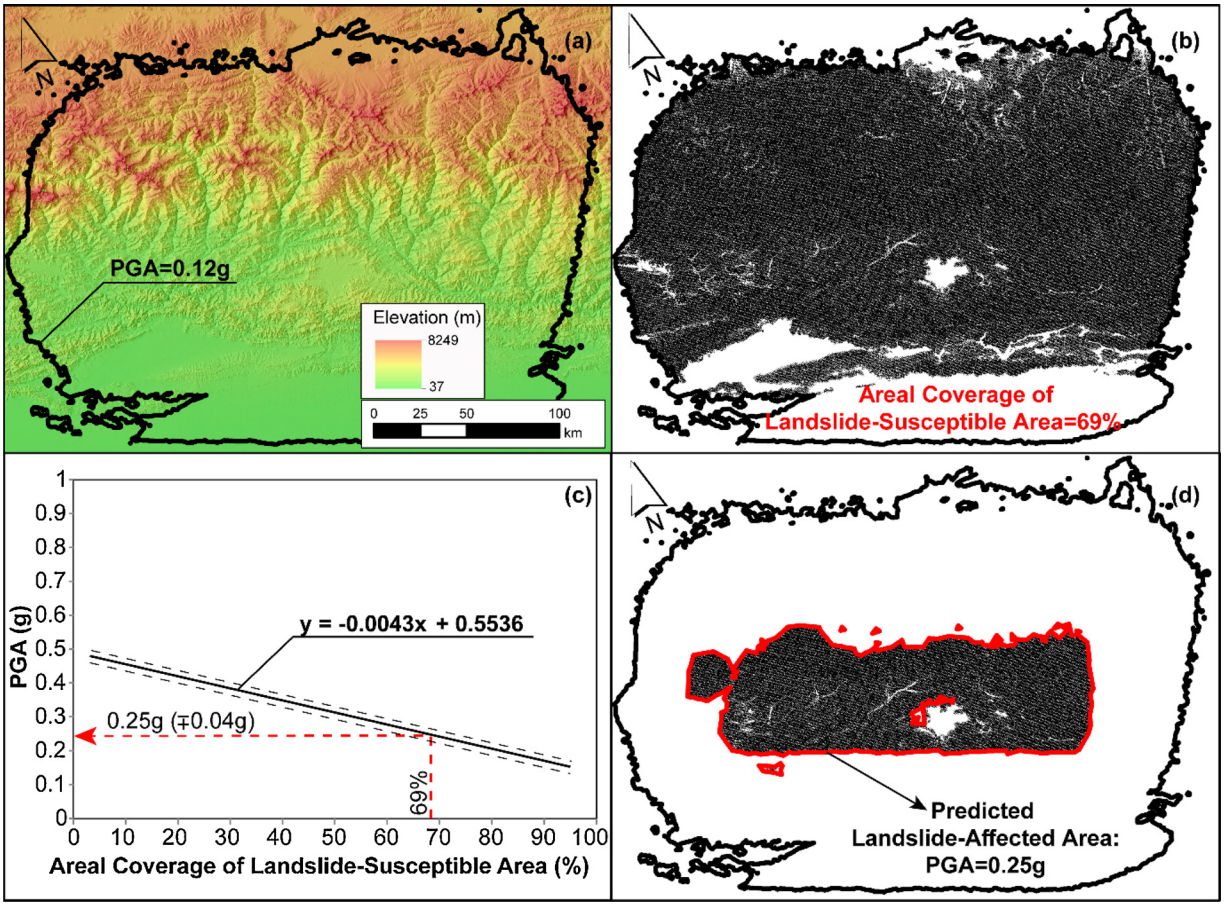

Fig. 3. The 2015 Gorkha earthquake is shown as an example to estimate the landslide-affected area: *a*) Extent of the 0.12 g Common PGA (Tanyaş and Lombardo, 2019); *b*) Calculation of the ACLSA (normalizing the surface of Common PGA by the extent of susceptible terrains with slope > 5° and local relief > 100 m); *c*) Predicting the actual PGA contour which expresses the likely landslide-affected area via the relation shown in Fig. 2; and *d*) Likely landslide-affected area translated into map form.

6. Discussion

The main limitations of the method we propose here are inherited from Tanyaş and Lombardo (2019). In addition to those, in this work, we add another limitation coming from the thresholds used to classify both PLEA and rollover point. However, this is inevitable, especially in a globally applicable classification tool. The choice we have made to provide a simplified classification scheme originates from the need to reduce the several sources of uncertainties into few classes. For this reason, the tool converts our quantitative evaluation into a qualitative one. As a result, we have developed a semi-quantitative framework to evaluate the completeness level of EQIL inventories.

Notably, it is challenging to validate the results because most of the original data lacked the required information; nevertheless, we provide our interpretation below.

As a reference, we initially check five of the EQIL inventories, which were reported as the most comprehensive by (Harp et al., 2011). These inventories correspond to the 1976 Guatemala (Harp et al., 1981), 1983 Coalinga (Harp and Keefer, 1990), 1994 Northridge (Harp and Jibson, 1995, 1996), 1999 Chi-Chi (Liao and Lee, 2000) and 2008 Iwate-aMiyagi-Nairiku (Yagi et al., 2009) events. Our classification result is generally consistent with the comments provided by (Harp et al., 2011). We classify the 1976 Guatemala (Harp et al., 1981), the 1983 Coalinga (Harp and Keefer, 1990) and the 1994 Northridge (Harp and Jibson, 1995, 1996) inventories with High-Completeness (HC). However, we classify the 1999 Chi-Chi (Liao and Lee, 2000) inventory with Moderate-Completeness (MC) due to its rollover size higher than 500 m^2. Lee (2013) stated that the Chi-Chi inventory, provided by Liao and Lee (2000), was rapidly mapped after the earthquake for the whole of Taiwan. Notably, Lee (2013) updated this inventory a few years after the disaster. However, we did not get access to this updated version although we can expect their new version to have a smaller rollover point. Nevertheless, our MC classification for the inventory provided by Liao and Lee (2000) is reasonable, considering the post-disaster time constraints during which it was compiled. Also, our calculations return a Low Completeness (LC) for the 2008 Iwate-Miyagi-Nairiku. This is an unusual case. However, by checking the Fig. 1 in Yagi et al. (2009), what stands out the most is that the geomorphological map is exceptionally detailed within the area examined by the authors. Nevertheless, the authors do not specify if they examined a larger region. A low completeness indicates that the expected area affected by landslides could have been larger than the actual area investigated by the authors. Specifically, our PLEA is ~40%.

We assign the 1976 Friuli inventory (Govi, 1977) with low-completeness (MC). Among all the inventories we analyze, this inventory is the oldest one, mapped in 1977. Because we do not have detailed information about the mapping procedure of this inventory, we cannot validate our finding for this inventory. Because of the imagery resolution at that time, it could be possible that landslides were mapped up to a coarser rollover point.

There are five inventories (1989 Loma Prieta (McCrink, 2001), 2006 Kiholo Bay (Harp et al., 2014), 2008 Wenchuan (Tang et al., 2016), 2013 Lushan (*W-L* Li et al., 2013), 2015 Gorkha (Tanyaş et al., 2018)) for which landslides have initially been mapped only within a subset of the landslide-affected area. Our completeness evaluation assigns LC to those, as expected.

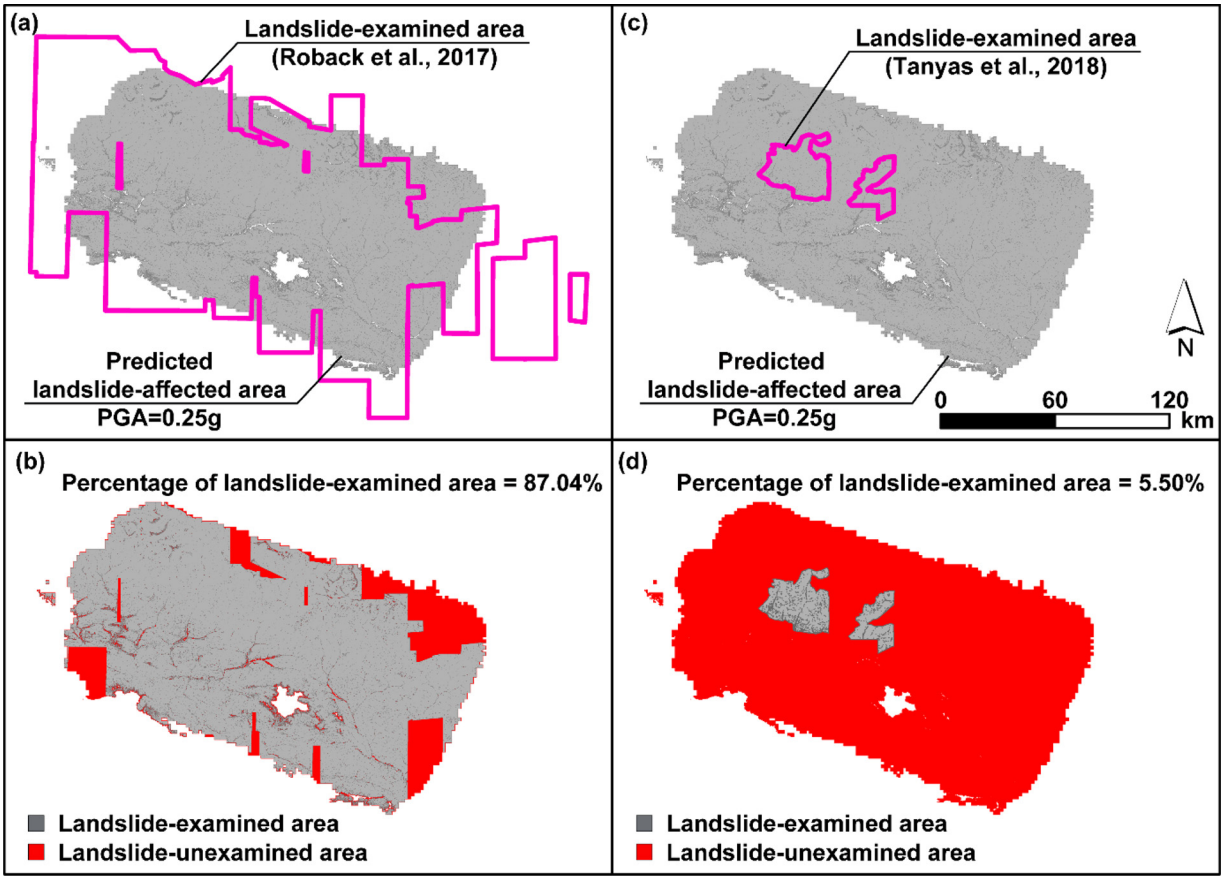

Fig. 4. Two independent examples for the 2015 Gorkha earthquake; *a*) and *b*) panels show how to compute the PLEA associated to the inventory provided Roback et al. (2017); panels *c*) and *d*) reflect the same operation for the inventory provided by Tanyaş et al. (2018). The polygons in magenta correspond to the respective landslide-examined areas.

For the 1991 Limon (Marc et al., 2016) and partially for the 2002 Denali (Gorum et al., 2014), inventories were provided using satellite imageries at a 30 m resolution. Our classification assigns an MC index, due to the respective rollover sizes, which are larger than 500m^2. In this regard, our classification result is consistent with our prior knowledge.

We classify the 1995 Hyogo-ken Nanbu inventory (Uchida et al., 2004) as LC. In this case, the authors of this inventory shared the landslide-examined boundary. Considering the small rollover size (65 m^2) for this inventory, overall we should assume it to be highly complete. However, our model uses the area encompassed by the 0.12 common PGA, which is larger than their surveyed area. This is the main reason why our result assigns a lower completeness index. We cannot test whether this is a limitation in our model, similarly to the Iwate-Miyagi case, or if more landslides may have actually been triggered in 1995 outside the landslide-examined boundary.

As for the 2005 Kashmir earthquake, we got access to three inventories (Basharat et al., 2016; Basharat et al., 2014; Sato et al., 2007) which we classify as LC. Among these, the estimated PLEAs are 28.32% (+6.28 & -6.83) and 10.69% (+2.37 & -2.58) and 16.21% (+3.6 & -3.91) corresponding to the inventories provided by Sato et al. (2007), Basharat et al. (2014) and Basharat et al. (2016), respectively. Basharat et al. (2016) stated that the first two inventories were provided over a minimal area; thus, we can justify the inferred LC. As for the LC index for the remaining inventory, we do not have access to the area surveyed by the authors (like for Iwate-Miyagi and Hyogo-ken Nanbu). More generally, this could still be due to our model uncertainty, as described in Tanyaş and Lombardo (2019).

In the case of the 2008 Wenchuan earthquake, we test four inventories. Three out of the four cover more than half of the landslide-affected area. Specifically, the estimated PLEA are 77.53% (+7.03 & -8.73), 97.36% (+1.02 & -5.86), and 63.53% (+4.62 & -7.02) for the inventories provided by Dai et al. (2011), Xu et al. (2014b), and *G* Li et al. (2014), respectively. However, the rollover points are larger than 500 m^2 for each inventory which results in an MC completeness index. Among the four, the inventory provided by Xu et al. (2014b) includes 197481 landslides over $8{\cdot}10^4$ km^2 which makes it the most comprehensive inventory for the Wenchuan earthquake. Nevertheless, small landslides might still be missing in this inventory. But also, one should consider that due to the numerous failures, the signature of small landslides could have been merged into a larger landslide body. Therefore, during the mapping procedure, it would have been challenging, for such a large landslide-affected area, to disentangle small from large mass movements.

The fourth inventory corresponds to the one presented in Tang et al. (2016). This inventory was prepared with great detail using post-disaster images acquired through drone surveys, but for a limited part of the landslide-affected area. The resulting PLEA is 0.48% (+0.11 & -0.12), which resulted in an LC index. We used the inventory provided by Tang et al. (2016) as a reference to validate the CI assigned to the other three. The comparison shows that the rollover point, associated with the inventory compiled by Tang et al. (2016), is much smaller than the ones estimated for the other three inventories, which cover a much larger region. As a result, we consider the MC assigned to the other three as acceptable.

We also examine the 2010 Haiti inventory presented by Harp and Jibson (2016). This is generally considered a complete inventory, with a considerable amount of small landslides mapped in detail (Tanyas et al., 2019). Based on our independent evaluation, this inventory is classified as HC. The inventory provided by Gorum et al. (2013) for the same earthquake is also classified as HC, although the PLEA is 84.85%

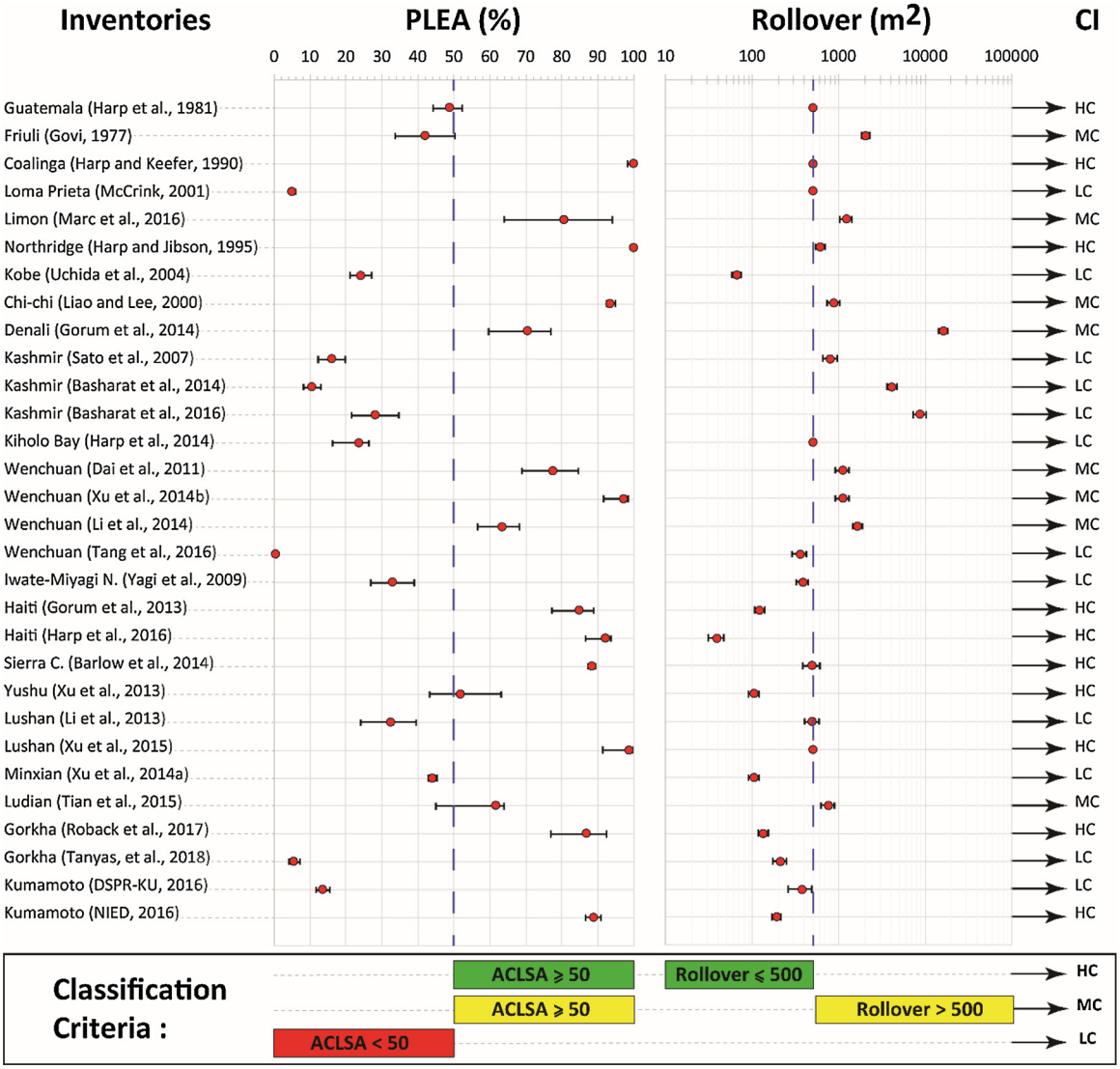

Fig. 5. This plot is arranged into 5 elements (four columns and 2 rows). The first column to the left lists each inventory and corresponding authors; The second columns shows the values we obtained for the Percentage of Landslide-Examined Area, whereas the third one reports the relative Rollover point estimates. The last column summarizes our proposed Completeness Index, whose classification criteria are graphically explained in the bottom row. The error bars correspond to the 95% credible interval of the regression model shown in Fig. 2 and described in Tanyaş and Lombardo (2019).

(+4.01 & -7.55). This is lower than the percentage obtained for Harp and Jibson (2016)'s inventory with a PLEA = 92.14% (+1.38 & -5.55).

Barlow et al. (2015) used SPOT 5 satellite imagery and mapped the landslides triggered by the 2010 Sierra Cucapah earthquake. Because the earthquake occurred in a mountain range restricted by alluvial fan surfaces, landslides would likely be triggered in a topographically restricted area. Barlow et al. (2015) mapped that region, and therefore, they most likely mapped the majority of landslides. Our CI evaluation is consistent with this observation for the inventory is classified as HC.

We classify the 2010 Yushu inventory of Xu et al. (2013) as HC. The authors used aerial photographs and satellite images to compile this inventory. The estimated PLEA is 51.95% (+11.28 & -8.82), which is just above the defined limit to be considered as HC. Therefore, the inventory can be considered at the transition between MC and HC.

Xu et al. (2015) mapped the landslides triggered by the 2013 Lushan earthquake and stated that they created a complete landslide inventory for this event. The result of our evaluation supports this argument for the inventory is classified as HC.

The PLEAs for the 2013 Minxian-Zhangxian (Xu et al., 2014a) and the 2014 Ludian (Xu et al., 2017) inventories are 44.09% (+1.22 & -1.17) and 61.81% (+2.01 & -16.92), respectively. We can consider the completeness class of Minxian-Zhangxian inventory as a transition between LC to MC. The Ludian inventory is MC just because of the coarse rollover point, although the actual value is very close to the 500m^2 reference (see Fig. 5).

We also estimate the completeness of the 2015 Gorkha (Roback et al., 2017) inventory to be HC. In this inventory, a very large area was surveyed (see Fig. 3, panels *a* and *b*), and landslides were mapped in such detail that source and deposits of landslides have been differentiated. Therefore, the obtained completeness class is consistent with our prior knowledge. For the same earthquake, the inventory compiled by *Tanyas et al. (2018)* is assigned with a LC index, which does not come as a surprise considering the mapped area (see Fig. 3, panels *c* and *d*).

We have two landslide inventories associated with the 2016 Kumamoto earthquakes. The first one (DSPR-KU, 2016) was released within one week from the mainshock, and thus it can be assumed not to include all landslides. Our approach classified this inventory as LC, which appears to be reasonable under the time constraints the authors had during the post-disaster phase. Conversely, the second inventory provided by NIED (2016) covered a much larger areal extent which has resulted in an HC index, also considering the relatively small rollover size.

These evaluations show that the proposed completeness classification leads to consistent results overall, each time being consistent with our classification-independent and prior knowledge of the mapping procedures. However, there are two sources of uncertainty affecting our method.

The first uncertainty affects the estimation of landslide-affected areas. In Tanyaş and Lombardo (2019), two parameters have been chosen to define susceptible areas, namely, 'slope' and 'local relief'. However, it is a well-known fact that other factors contribute to slope instability (e.g., lithology, structural geology, land cover, and groundwater conditions). However, the dual rule based on slope and relief is meant to support global applications, and substantial improvement should be possible if susceptible slopes are recognized via case-specific landslide susceptibility (Amato et al., 2019; Castro Camilo et al., 2017) or intensity (Lombardo et al., 2018; Lombardo et al., 2019b) analyses. The second weakness is due to missing landslide-examined boundaries. When the authors do not provide those boundaries, we fit a polygon covering all the mapped landslides and use this as a proxy for the actual surveyed region. In some cases, this approach can cause an underestimation of the completeness level because it is possible that a larger area was originally surveyed, but no further landslides were found.

7. Conclusions

This research aims at developing a CI-based method to estimate the level of completeness for EQIL inventories. The method considers the control of both topography and ground shaking on the initiation of EQIL (see Tanyaş and Lombardo, 2019). We introduce two proxies that correspond to the minimum fully-mapped landslide size (rollover point) and the ratio between the areal coverage of the examined region over the entire landslide-affected area (PLEA). We use the FAD of landslide inventories to derive the former proxy. And, we use two polygonal features pertaining to the mapping procedure and the actual extent of the landsliding process for the latter proxy. Since the EQIL are triggered as a result of a number of interplaying factors, the result of our numerical completeness evaluation is not necessarily devoid from uncertainties. On the contrary, substantial improvements can still be made by assessing the landslide-prone conditions in each inventory at a much higher resolution. However, even at the coarser level at which we have tested our method, we have classified each inventory with very reasonable CIs. And, an improvement from a qualitative to a (semi-) quantitative completeness evaluation was lacking in the geomorphological/engineering literature, making our workflow a useful tool to examine any EQIL inventory.

We believe that the proposed methodology can help researchers to be more aware of the limitations of EQIL inventories. As a result, considerations could arise on the basic requirements of open-access inventories. Also, in line with the purpose of the study, researchers may prioritize working on a specific dataset by relying on a numerical completeness measure. In our view, this method could become a standard requirement for any landslide study. Landslide models distributed over space will inherit some properties which reflect the completeness of the inventory. For instance, considering a smaller area than the theoretical landslide-affected area may emphasize some landscape properties or causative factors rather than others. In other words, an inventory with a low CI would inevitably either affect the considered absence locations (PLEA criterion) or train the model with a bias on the actual presences (Rollover criterion). This could be accounted for by associating the Completeness Index to the landslide susceptibility study. Also, studies focused on landscape evolution typically use the landslide volume information as one of the parameters. This is usually retrieved thanks to an area-to-volume conversion, but, a low CI would imply that the overall deposition budget would be possibly lower than the real one.

Ultimately, we provide the toolbox we developed to automatize the completeness assessment in the supplementary material. We hope that this would trigger a more standardized approach to estimate the completeness of an inventory both from the user and the mapper sides. The toolbox does not have a user manual, but every input/output window after launching the "CI" file contains detailed explanations and reference to the appropriate literature. We also share a test dataset to give the readers the chance to understand the required data structure and the report files produced at the end of the process. We tested it for all the considered inventories and the computational times ranged between 5 and 10 minutes (from the smallest to the most extensive inventories).

Declaration of Competing Interest

We hereby declare that the data we have used as well as the analyses and the manuscript we produce has no conflict of interest of any sort.

Appendix A. Supplementary data

Supplementary data associated with this article can be found, in the online version, at http://dx.doi.org/10.1016/j.enggeo.2019.105331.

References

Amato, G., Eisank, C., Castro-Camilo, D., Lombardo, L., 2019. Accounting for covariate distributions in slope-unit-based landslide susceptibility models. A case study in the alpine environment. Engineering geology 260, 105237. https://doi.org/10.1016/j.enggeo.2019.105237.

Barlow, J., Barisin, I., Rosser, N., Petley, D., Densmore, A., Wright, T., 2015. Seismically-induced mass movements and volumetric fluxes resulting from the 2010 Mw = 7.2 earthquake in the Sierra Cucapah, Mexico. Geomorphology. https://doi.org/10.1016/j.geomorph.2014.11.012.

Basharat, M., Ali, A., Jadoon, I.A., Rohn, J., 2016. Using PCA in evaluating event-controlling attributes of landsliding in the 2005 Kashmir earthquake region, NW Himalayas, Pakistan. Natural Hazards 81 (3), 1999–2017. https://doi.org/10.1007/s11069-016-2172-9.

Basharat, M., Rohn, J., Baig, M.S., Khan, M.R., 2014. Spatial distribution analysis of mass movements triggered by the 2005 Kashmir earthquake in the Northeast Himalayas of Pakistan. Geomorphology 206, 203–214. https://doi.org/10.1016/j.geomorph.2013.09.025.

Castro Camilo, D., Lombardo, L., Mai, P.M., Dou, J., Huser, R., 2017. Handling high predictor dimensionality in slope-unit-based landslide susceptibility models through LASSO-penalized Generalized Linear Model. Environmental Modelling & Software 97, 145–156. https://doi.org/10.1016/j.envsoft.2017.08.003.

Dai, F., Xu, C., Yao, X., Xu, L., Tu, X., Gong, Q., 2011. Spatial distribution of landslides triggered by the 2008 Ms 8.0 Wenchuan earthquake, China. Journal of Asian Earth Sciences 40 (4), 883–895. https://doi.org/10.1016/j.jseaes.2010.04.010.

DSPR-KU, 2016. Slope movement condition by 2016 Kumaoto earthquake in Minami-Aso village (as of 19:00 JST on 18 Apr 2016). Disaster Prevention Research Institute, Kyoto University (in Japanese). edited. http://www.slope.dpri.kyoto-u.ac.jp/disaster_reports/2016KumamotoEq/2016KumamotoEq2.html.

Fell, R., Corominas, J., Bonnard, C., Cascini, L., Leroi, E., Savage, W.Z., 2008. Guidelines for landslide susceptibility, hazard and risk zoning for land-use planning. Engineering Geology 102 (3-4), 99–111. https://doi.org/10.1016/j.enggeo.2008.03.014.

Ghosh, S., van Westen, C.J., Carranza, E.J.M., Jetten, V.G., Cardinali, M., Rossi, M., Guzzetti, F., 2012. Generating event-based landslide maps in a data-scarce Himalayan environment for estimating temporal and magnitude probabilities. Engineering geology 128, 49–62. https://doi.org/10.1016/j.enggeo.2011.03.016.

Gorum, T., Korup, O., van Westen, C.J., van der Meijde, M., Xu, C., van der Meer, F.D., 2014. Why so few? Landslides triggered by the 2002 Denali earthquake, Alaska. Quaternary Science Reviews 95, 80–94. https://doi.org/10.1016/j.quascirev.2014.04.032.

Gorum, T., van Westen, C.J., Korup, O., van der Meijde, M., Fan, X., van der Meer, F.D., 2013. Complex rupture mechanism and topography control symmetry of mass-wasting pattern, 2010 Haiti earthquake. Geomorphology 184, 127–138. https://doi.org/10.1016/j.geomorph.2012.11.027.

Govi, M., 1977. Photo-interpretation and mapping of the landslides triggered by the Friuli earthquake (1976). Bulletin of the International Association of Engineering Geology-Bulletin de l'Association Internationale de Géologie de l'Ingénieur 15 (1), 67–72. https://doi.org/10.1007/BF02592650.

Guzzetti, F., Malamud, B.D., Turcotte, D.L., Reichenbach, P., 2002. Power-law correlations of landslide areas in central Italy. Earth and Planetary Science Letters 195 (3), 169–183. https://doi.org/10.1016/S0012-821X(01)00589-1.

Guzzetti, F., Mondini, A.C., Cardinali, M., Fiorucci, F., Santangelo, M., Chang, K.-T., 2012. Landslide inventory maps: New tools for an old problem. Earth-Science Reviews 112 (1), 42–66. https://doi.org/10.1016/j.earscirev.2012.02.001.

Harp, E.L., Hartzell, S.H., Jibson, R.W., Ramirez-Guzman, L., Schmitt, R.G., 2014. Relation of Landslides Triggered by the Kiholo Bay Earthquake to Modeled Ground

Motion. Bulletin of the Seismological Society of America 104 (5), 2529–2540. https://doi.org/10.1785/0120140047.
Harp, E.L., Jibson, R.W., 1995. inventory of landslides triggered by the 1994 Northridge. California earthquake: U.S. Geological Survey Open-File ReportRep., pp. 95–213.
Harp, E.L., Jibson, R.W., 1996. Landslides triggered by the 1994 Northridge, California earthquake. Bulletin of the Seismological Society of America 86 (1B), 319–332.
Harp, E.L., R.W. Jibson, and R.G. Schmitt (2016), map of landslides triggered by the January 12, 2010, Haiti earthquake: U.S. Geological Survey Scientific Investigations Map 3353, 15 p., 1 sheet, scale 1:150,000. https://pubs.er.usgs.gov/publication/sim3353., edited, doi:10.3133/sim3353.
Harp, E.L., Keefer, D.K., 1990. Landslides triggered by the earthquake in. In: In: Rymer, M.J., Ellsworth, W.L. (Eds.), The Coalinga, California, Earthquake of May 2, 1983" 1487. U.S. Geological Survey Professional Paper, pp. 335–347.
Harp, E.L., Keefer, D.K., Sato, H.P., Yagi, H., 2011. Landslide inventories: The essential part of seismic landslide hazard analyses. Engineering Geology 122 (1-2), 9–21. https://doi.org/10.1016/j.enggeo.2010.06.013.
Harp, E.L., Wilson, R.C., Wieczorek, G.F., 1981. Landslides from the February 4, 1976, Guatemala earthquake. U.S. Geological Survey Professional Paper 1204-A, Washington, pp. 35 2 platesRep.
Keefer, D.K., 1984. Landslides caused by earthquakes. Geological Society of America Bulletin 95 (4), 406–421 doi:https://pubs.er.usgs.gov/publication/70014049.
Lee, C.-T., 2013. Re-Evaluation of Factors Controlling Landslides Triggered by the 1999 Chi–Chi Earthquake. In: Ugai, K., Yagi, H., Wakai, A. (Eds.), Earthquake-Induced Landslides: Proceedings of the International Symposium on Earthquake-Induced Landslides. Kiryu, Japan, 2012. Springer Berlin Heidelberg, Berlin, Heidelberg, pp. 213–224. https://doi.org/10.1007/978-3-642-32238-9_22.
Li, G., West, A.J., Densmore, A.L., Jin, Z., Parker, R.N., Hilton, R.G., 2014. Seismic mountain building: Landslides associated with the 2008 Wenchuan earthquake in the context of a generalized model for earthquake volume balance, Geochemistry, Geophysics. Geosystems 15 (4), 833–844. https://doi.org/10.1002/2013GC005067.
Li, W.-l., Huang, R.-q., Xu, Q., Tang, C., 2013. Rapid susceptibility mapping of co-seismic landslides triggered by the 2013 Lushan Earthquake using the regression model developed for the 2008 Wenchuan Earthquake. Journal of Mountain Science 10 (5), 699–715. https://doi.org/10.1007/s11629-013-2786-2.
Liao, H.-W., Lee, C.-T., 2000. Landslides triggered by the Chi-Chi earthquake. paper presented at Proceedings of the 21st Asian conference on remote sensing.
Lombardo, L., Mai, P.M., 2018. Presenting logistic regression-based landslide susceptibility results. Engineering Geology 244, 14–24. https://doi.org/10.1016/j.enggeo.2018.07.019.
Lombardo, L., Opitz, T., Huser, R., 2018. Point process-based modeling of multiple debris flow landslides using INLA: an application to the 2009 Messina disaster. Stochastic Environmental Research and Risk Assessment 32 (7), 2179–2198. https://doi.org/10.1007/s00477-018-1518-0.
Lombardo, L., Bakka, H., Tanyas, H., van Westen, C., Mai, P.M., Huser, R., 2019a. Geostatistical modeling to capture seismic-shaking patterns from earthquake-induced landslides. Journal of Geophysical Research: Earth Surface 124. https://doi.org/10.1029/2019JF005056.
Lombardo, L., Opitz, T., Huser, R., 2019b. Numerical Recipes for Landslide Spatial Prediction Using R-INLA: A Step-by-Step Tutorial. Spatial Modeling in GIS and R for Earth and Environmental Sciences. Elsevier, pp. 55–83. https://doi.org/10.1016/B978-0-12-815226-3.00003-X.
Malamud, B.D., Turcotte, D.L., Guzzetti, F., Reichenbach, P., 2004. Landslide inventories and their statistical properties. Earth Surface Processes and Landforms 29 (6), 687–711. https://doi.org/10.1002/esp.1064.
Marc, O., Hovius, N., Meunier, P., Gorum, T., Uchida, T., 2016. A seismologically consistent expression for the total area and volume of earthquake-triggered landsliding. Journal of Geophysical Research: Earth Surface 121 (4), 640–663. https://doi.org/10.1002/2015JF00373.
McCrink, P.T., 2001. Regional Earthquake-Induced Landslide Mapping Using Newmark Displacement Criteria, Santa Cruz County, California. In: In: Ferriz, H., Anderson (Eds.), Engineering Geology Practice in Northern California 210. Association of Engineering Geologists Special Publication 12, California Geological Survey Bulletin, pp. 77–93.
NIED, 2016. Distribution map of mass movement by the 2016 Kumamoto earthquake, edited by National Research Institute for Earth Science and Disaster of Japan. (in Japanese). http://www.bosai.go.jp/mizu/dosha.html.
Parker, R., Hancox, G., Petley, D., Massey, C., Densmore, A., Rosser, N., 2015. Spatial distributions of earthquake-induced landslides and hillslope preconditioning in the northwest South Island, New Zealand. Earth Surface Dynamics 3 (4), 501–525. https://doi.org/10.5194/esurf-3-501-2015.
Pelletier, J.D., Malamud, B.D., Blodgett, T., Turcotte, D.L., 1997. Scale-invariance of soil moisture variability and its implications for the frequency-size distribution of landslides. Engineering Geology 48 (3-4), 255–268. https://doi.org/10.1016/S0013-7952(97)00041-0.
Pellicani, R., Spilotro, G., 2015. Evaluating the quality of landslide inventory maps: comparison between archive and surveyed inventories for the Daunia region (Apulia, Southern Italy). Bulletin of Engineering Geology and the Environment 74 (2), 357–367. https://doi.org/10.1007/s10064-014-0639-z.
Roback, K., M. K. Clark, A. J. West, D. Zekkos, G. Li, S. F. Gallen, D. Champlain, and J. W. Godt (2017), Map data of landslides triggered by the 25 April 2015 Mw 7.8 Gorkha, Nepal earthquake: U.S. Geological Survey data release, doi:https://doi.org/10.5066/F7DZ06F9.
Rymer, M.J., 1987. The San Salvador earthquake of October 10, 1986-geologic aspects. Earthquake Spectra 3 (3), 435–463. https://doi.org/10.1193/1.1585440.
Sato, H.P., Hasegawa, H., Fujiwara, S., Tobita, M., Koarai, M., Une, H., Iwahashi, J., 2007. Interpretation of landslide distribution triggered by the 2005 Northern Pakistan earthquake using SPOT 5 imagery. Landslides 4 (2), 113–122. https://doi.org/10.1007/s10346-006-0069-5.
Schmitt, R.G., Tanyas, H., Jessee, M.A.N., Zhu, J., Biegel, K.M., Allstadt, K.E., Jibson, R.W., Thompson, E.M., van Westen, C.J., Sato, H.P., Wald, D.J., Godt, J.W., Gorum, T., Xu, C., Rathje, E.M., Knudsen, K.L., 2017. An open repository of earthquake-triggered ground-failure inventories. U.S. Geological Survey Data Series 1064.
Stark, C.P., Hovius, N., 2001. The characterization of landslide size distributions. Geophysical Research Letters 28 (6), 1091–1094. https://doi.org/10.1029/2000GL008527.
Tang, C., Westen, C.J.V., Tanyaş, H., Jetten, V.G., 2016. Analyzing post-earthquake landslide activity using multi-temporal landslide inventories near the epicentral area of the 2008 Wenchuan earthquake. Natural Hazards and Earth System Sciences 16 (12), 2641. https://doi.org/10.5194/nhess-16-2641-2016. 2016.
Tanyaş, H., et al., 2017. Presentation and Analysis of a World-Wide Database of Earthquake-Induced Landslide Inventories. Journal of Geophysical Research: Earth Surface 122 (10), 1991–2015. https://doi.org/10.1002/2017JF004236.
Tanyaş, H., Allstadt, K.E., van Westen, C.J., 2018. An updated method for estimating landslide-event magnitude. Earth Surface Processes and Landforms 43 (9), 1836–1847. https://doi.org/10.1002/esp.4359.
Tanyaş, H., Westen, C.J., Allstadt, K.E., Jibson, R.W., 2019. Factors controlling landslide frequency-area distributions. Earth Surface Processes and Landforms 44, 900–917. https://doi.org/10.1002/esp.4543.
Tanyaş, H., Lombardo, L., 2019. Variation in landslide-affected area under the control of ground motion and topography. Engineering Geology 260, 105229. https://doi.org/10.1016/j.enggeo.2019.105229.
Uchida, T., Kataoka, S., Iwao, T., Matsuo, O., Terada, H., Nakano, Y., Sugiura, N., Osanai, N., 2004. A study on methodology for assessing the potential of slope failures during earthquakes. Technical Note of National Institute for Land and Infrastructure Management, No.204, pp. 91p. (in Japanese with English abstract). http://www.nilim.go.jp/lab/bcg/siryou/tnn/tnn0204.html.
Van Den Eeckhaut, M., Poesen, J., Govers, G., Verstraeten, G., Demoulin, A., 2007. Characteristics of the size distribution of recent and historical landslides in a populated hilly region. Earth and Planetary Science Letters 256 (3-4), 588–603. https://doi.org/10.1016/j.epsl.2007.01.040.
Van Westen, C.J., Castellanos, E., Kuriakose, S.L., 2008. Spatial data for landslide susceptibility, hazard, and vulnerability assessment: an overview. Engineering geology 102 (3-4), 112–131. https://doi.org/10.1016/j.enggeo.2008.03.010.
Wasowski, J., Keefer, D.K., Lee, C.T., 2011. Toward the next generation of research on earthquake-induced landslides: current issues and future challenges. Engineering Geology 122 (1-2), 1–8. https://doi.org/10.1016/j.enggeo.2011.06.001.
Xu, C., Xu, X., Yu, G., 2013. Landslides triggered by slipping-fault-generated earthquake on a plateau: An example of the 14 April 2010, Ms 7.1, Yushu, China earthquake. Landslides 10 (4), 421–431. https://doi.org/10.1007/s10346-012-0340-x.
Xu, C., Xu, X., Shyu, J.B.H., Zheng, W., Min, W., 2014a. Landslides triggered by the 22 July 2013 Minxian–Zhangxian, China, Mw 5.9 earthquake: Inventory compiling and spatial distribution analysis. Journal of Asian Earth Sciences 92, 125–142. https://doi.org/10.1016/j.jseaes.2014.06.014.
Xu, C., Xu, X., Yao, X., Dai, F., 2014b. Three (nearly) complete inventories of landslides triggered by the May 12, 2008 Wenchuan Mw 7.9 earthquake of China and their spatial distribution statistical analysis. Landslides 11 (3), 441–461. https://doi.org/10.1007/s10346-013-0404-6.
Xu, C., Xu, X., Shyu, J.B.H., 2015. Database and spatial distribution of landslides triggered by the Lushan, China Mw 6.6 earthquake of 20 April 2013. Geomorphology 248, 77–92. https://doi.org/10.1016/j.geomorph.2015.07.002.
Xu, Chong, Xu, Xiwei, Shen, L., Dou, S., Wu, S., Tian, Y., Li, X., 2017. inventory of landslides triggered by the 2014 Ms 6.5 Ludian earthquake. https://doi.org/10.5066/F7QJ7FTF.
Yagi, H., Sato, G., Higaki, D., Yamamoto, M., Yamasaki, T., 2009. distribution and characteristics of landslides induced by the Iwate–Miyagi Nairiku Earthquake in 2008 in Tohoku District, Northeast Japan. Landslides 6 (4), 335–344. https://doi.org/10.1007/s10346-009-0182-3.